UNIVERSITY OF CALIFORNIA
SANTA CRUZ

MESOSCALE EDDIES IN THE GULF OF ALASKA: OBSERVATIONS AND IMPLICATIONS

A dissertation submitted in partial satisfaction of the
requirements for the degree of

MASTER OF SCIENCE

in

OCEAN SCIENCES

by

Peter Rovegno

December 2012

The Dissertation of Peter Rovegno
is approved:

Professor Christopher A. Edwards, Chair

Professor Kenneth W. Bruland

Professor Raphael Kudela

Tyrus Miller
Vice Provost and Dean of Graduate Studies

Table of Contents

List of Figures

List of Tables

Abstract

Mesoscale Eddies in the Gulf of Alaska: Observations and Implications

by

Peter Rovegno

Mesoscale eddies in the Gulf of Alaska are thought to contribute to the shelf-slope exchange of nutrients and plankton, enhancing biological production. We report on a study of two anticyclonic mesoscale eddies in this region observed through in situ sampling during August and September 2007. Both eddies exhibited in their cores θ-S profiles with warmer, fresher water relative to the properties of the ambient basin water between 150 and 300 m depth. Hydrographic properties and satellite altimetry data were analyzed to identify likely formation regions for each feature. One eddy, sampled near Yakutat, Alaska, originated in the Sitka formation region ($221-223^\circ$ E); the second eddy, sampled south of Kodiak Island, originated near the Kenai Peninsula, southeast of the Kennedy and Stevenson entrances to Cook Inlet — an area not previously studied as a formation region. Subsequent analysis of 16 years of satellite altimeter data (from 1992 to 2008) with an algorithm designed to identify and track eddies revealed approximately 6 Kenai eddies that have formed in this region. Although this number constitutes only 3.2% of the 188 eddies identified by the algorithm during this period, it represents 15.4% of the 39 eddies that formed in or propagated westward into the Alaskan Stream.

Acknowledgments

The text of this thesis includes reprints of the following previously published material: [*Rovegno et. al*(2009)]. The co-authors listed in this publication directed and supervised the research which forms the basis for the thesis.

Chapter 1

Introduction

The coastal region of the Gulf of Alaska (GoA) is considered one of the most productive zones of the west coast of North America, despite the downwelling-favorable conditions that prevail over most of the year. The primary circulation in the GoA is the wind-forced subpolar gyre, which is bounded to the south by the eastward-flowing North Pacific Current (Figure 5.1). The North Pacific Current bifurcates into poleward and equatorward-flowing branches off the coast of North America, and the northern branch, known as the Alaskan Current, forms the eastern boundary of the gyre. The Alaskan Current flows northwest, and begins to narrow and strengthen as it passes the head of the Gulf, near the entrance to Prince William Sound. Past this point, the current closely follows the shelf break to the southwest and is referred to as the Alaskan Stream, the western boundary current for the gyre, which can flow at speeds of up to 90 cm/sec (Stabeno & Reed (1991)). Further to the southwest, out along the Aleutian Chain, some Alaskan Stream water rejoins the North Pacific Current. In addition, a

buoyancy-driven coastal flow, known as the Alaskan Coastal Current, flows along the shoreward side of the shelf break. The Alaskan Coastal Current is thought to begin to the southeast of Prince William Sound, propagates to the southwest along the Kenai Peninsula, and then continues to Shelikov Strait on the landward side of Kodiak Island via the Kennedy and Stevenson entrances to Cook Inlet (Stabeno *et al.* (2004)).

Superimposed on the general circulation pattern, there are typically several anticyclonic mesoscale eddies present in the GoA at any given time (Henson & Thomas (2008)). These eddies form on or near the shelf, typically range from 80 to 200 km in diameter, and possess cores with baroclinic structure that extend to depths of $\sim$ 1500 m or below (Tabata (1982), Crawford (2002)). This core water is usually fresher, warmer, and nutrient-rich relative to ambient basin water in the same depth range (Peterson *et al.* (2005), Ladd *et al.* (2005)).

Although the supply of macronutrients on the shelf is somewhat limited by the downwelling-favorable winds, micronutrients (such as iron) are suggested to be abundantly supplied by riverine inputs and resuspension of sediments (Stabeno *et al.* (2004)). In contrast, the interior of the GoA is known to be an iron-limited, high-nutrient, low chlorophyll (HNLC) zone (Martin *et al.* (1989)). The iron limitation of phytoplankton in the central GoA has been further reported on by Boyd *et al.* (2005) and also La Roche *et al.* (1996), who contrasted the severe iron stress evidenced by basin phytoplankton with the lack of iron stress evidenced by coastal phytoplankton. Bathymetric gradients inhibit mean cross-shelf transport, segregating coastal iron from the basin and maintaining the HNLC zone in the interior of the GoA. Mesoscale eddies play an important

role disrupting mean alongshore flow and enhancing shelf-slope exchange when they propagate along the shelf break (Whitney & Robert (2002), Johnson *et al.* (2005)). The leading edge of the eddy entrains macronutrient-rich basin water while the trailing edge entrains iron-rich shelf water, inducing a net nutrient exchange between the basin and shelf waters (Okkonen *et al.* (2003), Whitney *et al.* (2005)). Additionally, as the eddies age and decay, there is a gradual release of their shelf-break-originated core waters to the surrounding basin.

The effect of the entrainment and mixing of water masses by eddies on biological productivity can be seen in satellite maps of chlorophyll concentration. For instance, in those presented by Okkonen *et al.* (2003) (their Figure 1), plumes of high productivity can be seen wrapping around the edges of two mesoscale eddies in the GoA. These blooms of productivity are thought to result from the mixing of the iron-rich entrained shelf water with the iron-limited (but macronutrient-rich) waters of the interior of the GoA.

The knowledge of physical properties, formation mechanisms, and influence of eddies on the GoA has mostly been derived from observations of those features that form in the eastern Gulf, categorized by the geographical location of their generation regions as either Haida, Sitka, or Yakutat eddies. Haida eddies, first observed by Kirwan *et al.* (1978), form on an annual basis in the vicinity of Queen Charlotte Island (between 226 and 229° E), likely due to strong outflow past the southern point of the island (Di Lorenzo *et al.* (2005)). Haida eddies typically move westward into the basin interior (Crawford (2002)), although a number will propagate a short distance to the northwest

along the shelf-break before detaching. The role of Haida eddies in transporting shelf water and biota into the interior of the GoA has been well-documented from a wide spread of sampled eddies (Mackas & Galbraith (2002), Crawford *et al.* (2002), Whitney & Robert (2002)), and further verified by analysis of ocean color data from satellites (Crawford *et al.* (2005)).

Sitka eddies, first observed by Tabata (1982), form in the winters of most years off of the narrow shelf near Sitka, Alaska (between 221 and 224° E). A variety of formation mechanisms have been proposed, ranging from atmospherically-forced planetary waves to interaction of the Alaskan Current with bathymetry to reversals in the southeasterly wind forcing along the coast in that region (Willmott & Mysak (1980), Swaters & Mysak (1985), Thomson & Gower (1998)). Many Sitka eddies detach from the shelf and travel westward into the interior of the Gulf (Matthews *et al.* (1992)), although some propagate to the northwest along the shelf-break, eventually rounding the head of the Gulf to become embedded in the Alaskan Stream (Crawford *et al.* (2000)). Sitka eddies, like Haida eddies, have also been seen to transport high-chlorophyll waters off the shelf in satellite images of ocean color (Crawford *et al.* (2005)).

The third type, Yakutat eddies, form in the winter off of the wide shelf between Kayak Island and the region southwest of Yakutat Bay ($216 - 219°$ E) (Ladd *et al.* (2005)). Yakutat eddies usually travel west past the head of the Gulf, becoming embedded in and propagating to the southwest with the Alaskan Stream (Ladd *et al.* (2007)). The mechanisms for generating Yakutat eddies are generally thought to be similar to those responsible for Sitka eddies. The transport of shelf water in the core

of Yakutat eddies has been observed and reported by Musgrave *et al.* (1992) and Ladd *et al.* (2005).

In addition to these observational studies that have focused on eastern formation sites, previous modeling studies have also noted the difference in eddy activity between the eastern and western GoA. Cummins & Mysak (1988) created a quasi-geostrophic model that was able to reproduce eddy-like features in the eastern Gulf, but produced only meanders in the Alaskan Stream. In a three-dimensional modeling study, Combes & Lorenzo (2007) found that eddy variability in the eastern GoA was extrinsically forced by atmospheric fluxes, whereas variability in the western GoA was intrinsic, and thus related to internal instabilities of the Alaskan Stream. A recent census of eddies by Henson & Thomas (2008), building on the work of Ladd *et al.* (2007), used an objective algorithm to identify eddies in the Alaskan Stream, but did not distinguish between eddies that had formed locally and those that formed in the eastern Gulf and transited westward into the Alaskan Stream region. The reasons for these differences between the eastern and western Gulf are still poorly understood.

The use of satellite altimetry to identify and track individual eddies has become more common in recent years (Crawford *et al.* (2000), Crawford *et al.* (2002), Crawford (2002), Ladd *et al.* (2005), Matthews *et al.* (1992), Okkonen *et al.* (2003)), but the application of satellite data to the analysis of eddy activity in the gulf as a whole, as in Ladd *et al.* (2007) and Henson & Thomas (2008), has only emerged within the last couple of years.

In this thesis, we describe hydrographic data taken from two eddies during a

cruise to the GoA in August and September, 2007. The subsequent analysis of this data, coupled with an examination of the satellite altimetry record using an objective eddy identification algorithm similar to that of Henson & Thomas (2008), leads us to identify one of the sampled eddies as a Sitka eddy. The other eddy appears to have originated during the winter in the area south of the Kenai Peninsula and east of Kodiak Island. This suggests that there may be a relatively unstudied formation region for eddies in the western Gulf, south of the Kenai Peninsula in the waters near the Kennedy and Stevenson entrances to Cook Inlet, and we suggest that these eddies be called Kenai Eddies.

In the years since the publication of our initial work, several groups have fleshed out our picture of this particular Kenai eddy: Ueno *et al.* (2012) measured the core water properties and tracked the propagation of the Kenai eddy out along the Aleutian Chain, where it was still extant through 2009; Lippiatt *et al.* (2011) examined the delivery of iron to the interior of the Gulf via mechanisms associated with the Kenai eddy; Fiechter *et al.* (2011) and Fiechter & Moore (2012) used modeling to examine iron limitation and physical-biological coupling mediated by eddies in the Gulf. The results of these particular studies and how they dovetail with several avenues of inquiry suggested by our work will be discussed in the Conclusion.

Chapter 2

Data

Data were collected using a Seabird SBE 911plus CTD, calibrated with IAPSO standard seawater, based off of the University of Washington vessel, *Thomas J. Thompson*, and was subsequently interpreted using MATLAB^{TM} scripting. Potential temperature was calculated from in situ values of temperature, salinity and pressure using the SEAWATER toolbox from CSIRO. Daily satellite altimetry estimates obtained from the Real-Time Altimetry Project at the Colorado Center for Astrodynamics Research (CCAR) were used to monitor sea surface height anomalies (SSHa) in the Gulf of Alaska during the cruise. These data, in conjunction with the shipboard ADCP, guided in situ sampling of the eddies. For post-cruise analysis and figures presented here, the Aviso Delayed-Time Global Sea Level Anomaly altimetry product was used. The Delayed-Time product is derived from the Ssalto/Duacs system, which combines data from the Jason-1, TOPEX/Poseidon, Envisat, GFO, Geosat, and ERS-1 & 2 altimeter missions. Cruise sampling was directed at two Gulf of Alaska eddies present during August 2007

— one off of the coast near Yakutat, Alaska (hereafter the "Sitka Eddy" based on its estimated formation zone to be described below) and a second off the coast of Kodiak Island (hereafter the "Kenai Eddy").

Table 5.1 summarizes key information from the CTD casts. There were 22 CTD casts taken in the vicinity of the Sitka Eddy from 21-Aug-2007 to 25-Aug-2007 (ID numbers 2 through 23). During this time the magnitude of the SSHa signature changed by less than 1 cm and the location of the eddy center, as determined below, changed by less than 7 km. The largest common depth for all casts (except for CTD casts 2 and 3, located on the shelf) was 300 m, although 10 of the casts were taken to 2000 m or below. Figure 5.2a shows the locations of these stations overlaid on a map of SSHa derived from the Aviso dataset from the time closest to when the measurements were taken (the Aviso product used is available as weekly-averaged snapshots), with values over land removed from the data. The north-east to south-west transect across the Sitka Eddy was sampled first, with the north-west branch of casts being taken after returning to the eddy center from the south.

From the altimetry, it is evident that two SSHa maxima exist in the northern part of the Gulf. Post cruise analysis reveals that the southern SSHa maximum originated as a lobe detaching from the more northern feature in early August 2007, weeks prior to the sampling. Hydrographic analysis, shown below, reveals that the northern SSHa maximum had clearly identifiable eddy core water properties, whereas the feature to the south had more mixed θ-S structure. Interestingly, the intensity of the southern feature subsequently grew whereas the more northern SSHa maximum decreased in

strength and dissappeared along the shelf.

Two transects across the Kenai eddy were taken over the period from 06-Sep-2007 to 10-Sep-2007, comprising 18 total CTD casts (ID numbers 34 through 51). The initial transect was approximately east-to-west, followed by a more north-to-south transect. During the course of sampling, the eddy center moved horizontally by less than 2 km, and the maximal internal SSHa value changed by less than 3 cm. With the exception of two on-shelf casts (CTD casts 44 and 45), those Kenai eddy stations were taken to a common depth of 1000 m (Table 5.1). The locations of these stations are shown in Figure 5.2b overlaid on the Aviso-derived altimetry map for 05-Sep-2007.

Both the Kenai and Sitka eddies had water properties similar to those of other GoA eddies recorded in the literature (Ladd *et al.* (2005), Tabata (1982)). The upper 75 m of the water column is characterized by a strong gradient in potential temperature, and this temperature gradient dominates the density variations. In contrast, deeper temperature structure in both eddies is characterized by an inversion, with a local maximum in the $200 - 300$ m range (Figure 5.3a,b). This maximum exceeded values of ambient fluid at these depths outside the eddy by approximately a degree. From our analysis of sea surface height described below, we believe that both eddies formed during the previous winter and that seasonal stratification makes the upper 75 m of the water column less representative of the eddy structure at formation than the more sheltered features beneath about 150 m. This conclusion is consistent with work by Suga *et al.* (2004), who report the depth of the winter mixed layer in the GoA as lying between 75 and 100 m. As a result, much of our analysis below focuses on the hydrographic

structure in this deeper portion of the upper water column. Note also that in Figure 5.3, the colormap for the temperature plots was truncated at 8°C, so as to emphasize the temperature structure below 75m. Stability of the water column in the vicinity of the temperature inversion is maintained by variations in salinity, and a strong halocline is present in the region (Figure 5.3c,d). Both isohalines and closely associated isopycnals (Figure 5.3e,f) are locally depressed within the eddy. Although the figures extend only to 300 m, data from deep CTD casts taken reveal bowing isopycnals to the deepest available depths for each eddy — 2000 m for the Sitka eddy and 1000 m for the Kenai eddy — consistent with observations by Crawford (2002) and Ladd *et al.* (2005) and indicating eddy structure extending over a sizeable fraction of the total water column.

As evident in both the surface SSHa maps and hydrography, both eddies are found close to the continental shelf break. The white region of no-data in Figure 5.3 indicates truncation of the CTD cast due to limited water depth at the station location. For the Sitka eddy, the edge of the anomalous water properties is found approximately 100 km from the nearest shelf cast (< 200 m). For the Kenai eddy, anomalous water properties appear to extend partially up into the shallow shelf region. This coincidence of the location of the eddy's edge and the shelf break is consistent with the region of high eddy probability found in Henson & Thomas (2008).

The magnitude of the SSHa expression for the Kenai and Sitka eddies lay in the $30-40$ cm range, which falls towards the higher end of the ranges reported by Henson & Thomas (2008) ($6.2-53.4$ cm for the Alaskan Stream region, with average 25.5 cm, and $2.5-49.2$ cm for the Yakutat and Sitka formation region, with average 19.3 cm), but

similar to the 40 cm maximum reported by Crawford (2002) for Haida and Sitka eddies. This SSHa, coupled with the sloping isopycnals, sets up the characteristic anticyclonic azimuthal geostrophic velocities that serve to define and maintain the eddy — both the Kenai and the Sitka eddies have maximal calculated surface geostrophic velocities in the $20 - 40$ cm/sec range. Okkonen *et al.* (2003) estimates azimuthal geostrophic velocities of 30 cm/sec and 40 cm/sec for the eddies observed in their study, while Ladd *et al.* (2005) reports velocities close to 20 cm/sec derived from drifters approximately 20 km from the eddy center during both of their 2003 transects of a Yakutat eddy. These values correspond well with our calculations, as the maximum azimuthal velocities for the sampled Kenai and Sitka eddies occur closer to 40 km from the eddy centers (defined for this purpose as the point along a transect where the sign of the azimuthal velocity changes). As of 23 January 2008, the last available SSHa data at the time of our analysis, the Kenai eddy was still in existence, while the Sitka eddy had dissipated in early December 2007.

Chapter 3

Analysis

Our goal in the paper is to diagnose eddy properties, identify formation regions, and characterize the paths of the two features sampled. We begin the analysis with a straightforward description of water masses in the vicinity of the two eddies. The θ-S structure provides excellent distinguising characteristics with which to isolate eddy core from adjacent casts, and also proves useful for identifying potential source regions for those cores. We then use the time-series of SSHa estimates from the altimeter to trace the eddies back in time to their approximate point of origin temporally and geographically, allowing a cross-check of the formation regions suggested by the hydrographic evidence.

3.1 Water masses

All hydrographic casts showed characteristic profiles consisting of warm, relatively fresh surface water, a deeper halocline, and increasingly cool and saline water at

depth. However, differences in their structure allowed straightforward categorization. This information was combined with geographical cast locations relative to the eddy edges as determined by altimetry in order to group casts into relevant subsets.

The Sitka eddy had four such subsets: basin water, core water, secondary core water, and transitional water. Casts 22 and 23 were classified as basin water (Figure 5.4a), characterized by comparatively saline surface water, a subsurface temperature minimum of 3.8°C near a salinity of 32.9, and a deeper temperature maximum of 4.9°C near salinity 33.7. Judging from altimetry, these two casts were taken outside of the eddy to the northwest. Casts 6, 8-11, 19, and 20 were located in the vicinity of the northern SSHa maximum for the eddy, and comprised the eddy core water (Figure 5.4b). They revealed less saline surface water relative to the basin casts, and water with temperatures in the range of $5.2 - 6.2$°C for salinities in the range of $32.6 - 33.7$. These profiles, just as those for the basin water, included a positive slope between subsurface temperature extrema, but at higher temperature and lower salinity (i.e., lower density). The secondary core water group consisted of casts 14-17 (Figure 5.4c), which were clustered around the southern local SSHa maximum of the Sitka eddy. The surface water for these casts had salinity values between those of the core water and basin water casts. The subsurface temperature inversion in these casts is much weaker than in either the core or basin waters. The properties at the top of the halocline (near density 25.8 kg/m^3) more closely resemble those of the core than basin casts, but the properties within the halocline are more scattered, suggesting increased water mass mixing at these salinities. Transitional water was identified in casts 5, 7, and 21, taken

both along the northwest and northeast edges of the eddy, between locations where core water and basin water were found (Figure 5.4d). Transitional water was characterized by more saline surface water than either core or secondary core water, while still being less saline than basin water. The temperature inversion for these casts is weak or non-existent, and the θ-S curve lies in the region between the core water and basin water properties.

The θ-S curves of the CTD casts for the Kenai eddy fell into only three separate groups — basin water, core water, and transitional water — as the Kenai eddy did not have the curious twin maxima of SSHa present in the Sitka eddy. Casts 42 and 49-51 were taken outside of the eddy to the south and west (respectively), and were classified as basin water (Figure 5.5a). Basin water was again characterized by comparatively saline water in the surface layer, and a positive slope connecting the subsurface temperature minimum of $3.5°C$ at salinity 32.8 with the deeper subsurface temperature maximum of 4.5°C at salinity 33.7. The core waters for the Kenai eddy were sampled by casts 35-39 and 45-47 (Figure 5.5b) from the east-west and north-south transects, respectively. Core θ-S profiles showed relatively little scatter, and the subsurface temperature inversion was found between 4.5 and 5.5°C with salinities in the $32.6 - 33.7$ range. Surface water was fresh relative to that of the basin water for these profiles. Casts 34, 40, 44, and 48 were identified as being transitional water, with θ-S properties between those of core and basin-water stations (Figure 5.5c). The surface layer was fresher than that of the basin water, but still more saline than that of the core water. There was a relatively narrow band ($4.8 - 5.2$°C) of temperatures occupied by the transitional water in the salinity

interval of $32.6 - 33.7$, with a more level slope of the θ-S profile than for the other two Kenai water groups. At the top of the halocline, the transitional water closely matched θ-S properties of core stations, but deeper fluid within the halocline suggests a mix of core and basin-properties. Altimetry reveals that these transitional casts occur near the edge of the Kenai eddy and between the locations of core and basin-water stations, consistent with the hydrography.

Between the Sitka and the Kenai eddy, we can see that, while the shapes of the θ-S profiles for their core water are quite similar, with a significant positive slope over the $32.6 - 33.7$ salinity range (Figure 5.6), the Kenai eddy core water is almost uniformly $0.7 - 1.0°$C colder in this range. Since water properties beneath the surface mixed layer are slowly modified, this difference in halocline temperature was taken as an indication that the sources of the eddy core water, and hence their formation regions, were different for each of the two eddies.

As an additional check, a comparison of the CTD casts for GoA basin water in the vicinity of each of the two eddies (Figure 5.7) shows that, while they also share a similarity in shape, the magnitude of the temperature difference between them is only about $0.3 - 0.4°$C. Although it is possible that the source regions for each of the two eddies were the same, and that the differences in the core water properties sampled are solely due to differential mixing with ambient basin water with unique θ-S properties, this scenario was considered unlikely when compared to that in which eddies formed in different locations with distinct θ-S properties.

θ-S properties from CTD casts taken more distantly from sampled eddies were

compared with those of the previously-identified eddy core water to identify likely source regions. Figure 5.8 shows the θ-S diagram for CTD cast 4 (blue triangles), taken at $(58.93°N, 218.94°E)$ to the northeast of the Sitka eddy on the shelf break (water depth $\sim$ 530 m, along with the θ-S properties of the Sitka core water (red dots). Below 6°C the agreement between the two sets of θ-S properties is excellent. Although the Sitka eddy formed 6 months prior, the similarity of the water properties in cast 4 to those of the eddy core is suggestive of a near-shelf formation location.

In order to check for error in our analysis of the altimetry data leading to an inaccurate identification of the eddy boundary (perhaps leading to the classification of cast 4 as being outside of the eddy, when it was actually inside the eddy boundary), we examined closely the hydrographic properties from geographically proximate CTD casts. Cast number 5, taken at $(58.796°N, 218.642°E)$ with θ-S properties shown in Figure 5.8 as green triangles, is located between cast 4 and cast 6 $(58.519°N, 218.034°E)$, the first of the casts previously identified as Sitka core water, and was placed in the "transitional" group discussed above. As the rotational sense of the eddy was anticyclonic, we expect that basin water from the west/northwest was entrained along the eddy edge at this point, and mixed with the eddy core water to result in the type of profile seen in cast 5. Having a cast with distinct θ-S properties between casts 4 & 6 reinforces the supposition that cast 4 lay outside the eddy boundary and that it is likely near the eddy formation region.

The station that had water properties most similar to those of the Kenai core water was the location where CTD cast 32 was taken: at $(58.677°N$, $209.453°E)$, in the

waters near the Amatouli Trough by the Kennedy Entrance to Cook Inlet, south of the Kenai Peninsula. Figure 5.9 shows the θ-S properties of cast 32 overlaid on those of the Kenai core water, with those of one of the "basin" casts (cast 49) shown for contrast. The agreement of the data between the Kenai core and cast 32 is excellent below the 5.3°C mark, but comparison is limited to the upper water column, as the cast could only be taken to 210 m before reaching the bottom. While the agreement of the θ-S properties is suggestive, the temporal separation of the data obtained from cast 32 with the actual time of eddy formation 6 months prior precludes using it as direct evidence of formation, and so we will rely on altimetry data to reinforce the hypothesis that this was near the source region for the core waters of the Kenai eddy. The locations of both cast 4 and cast 32 are marked in Figure 5.10 with a star and a triangle, respectively.

3.2 SSHa analysis

In order to understand the translation of the Sitka and Kenai eddies, including their formation and termination regions, we analyzed a time-series of SSHa estimates from Aviso. Since the surface expression of these mesoscale eddies is a persistent, coherent positive SSHa signal with significant vorticity, we used the satellite data to develop an algorithm to automatically identify and track eddy-like features within the GoA for the entire duration of the satellite record (1992 to 2008).

Our approach is a hybrid version of that used by Isern-Fontanet *et al.* (2003) and Henson & Thomas (2008) with that of Ladd *et al.* (2007). Specifically, we used both

the Okubo-Weiss parameter (W) and contours of sea surface height anomaly to identify eddy cores and boundaries and link them through time. The Okubo-Weiss parameter (W) is defined as

$$W = s_n^2 + s_s^2 - \zeta^2 \tag{3.1}$$

where ζ is the fluid relative vorticity, and s_s and s_n are the shear and normal strain, respectively. This diagnostic measure records the relative strength of vorticity and strain in a velocity field, and eddies are charactized by high vorticity in their center (i.e., $W < 0$) and high strain along their edges, where $W > 0$. Snapshots of SSHa were initially filtered by subtracting the spatial mean from each frame, generating new anomalies now relative to the time-varying larger-scale height field. Surface geostrophic velocities were calculated according to:

$$u = -\frac{g}{f}\frac{\partial \eta}{\partial y}, v = \frac{g}{f}\frac{\partial \eta}{\partial x} \tag{3.2}$$

where η is the filtered SSHa in meters, g is the gravitational constant, and f is the Coriolis parameter. Vorticity and strain components were determined from the geostrophic velocity field. A double threshold was used to identify eddies; we required Okubo-Weiss parameters with values less than a critical value $W_c = -0.2\sigma$ (where σ is the standard deviation of W in a snapshot) and whose filtered SSHa exceeded +10 cm as in Ladd *et al.* (2007). We chose the latter threshold in order to eliminate more transient features (that tended to have small SSHa amplitude) and select mostly long-lived eddies. The algorithm as described thus far identifies eddies within each snapshot. Eddy continuity through time was established by searching for unions of regions, defined by the +10

cm contour, from adjacent time frames and requiring $W < W_c$ somewhere within each region.

To avoid altimetric inaccuracies near land, features with centers in water depths less than 200 m were eliminated by our algorithm. As with Henson & Thomas (2008) a post-processing duration cut of 12 weeks was applied to eliminate short-lived features from the resultant eddy census. Despite our less stringent criteria for eddy identification, our tracking algorithm still suffers the same two issues noted by Henson & Thomas (2008) with their algorithm. Firstly, features tracked that fail to meet required thresholds for at least one timestep, but later strengthen are flagged as two separate eddies instead of one continuous one. Secondly, features that split into two or merge together are difficult to categorize simply. In our approach, features that divide are each identified by our algorithm, but the linkage to the parent structure is explicit only for the child eddy that shares the greatest overlapping area with the parent. In the case of splitting, this procedure may result in misattribution of formation location, and in the case of merging tracks, misattribution of termination location. Additionally, Chaigneau *et al.* (2008) found in a study of the Peruvian Current that the Okubo-Weiss method identified excess numbers of eddies relative to their winding angle method of eddy detection. However, upwards of 80% of the eddies detected in their study had durations of less than 12 weeks and low amplitudes, and thus would be eliminated by our requirement of 3 month eddy duration. We consider it likely that the majority of any false positives would fall into this category.

In total, we found 188 features in the record between October 1992 and January

2008. This number is larger than the 129 found by Henson & Thomas (2008) for a 1-year shorter record. This difference largely results from their use of the Okubo-Weiss parameter exclusively to define the eddy core region along with a requirement that eddies exceed an 80 km spatial scale. When we impose a similar constraint (area defined by $W < W_c$ exceeding 5000 km^2), we identify 126 features. We found that our hybrid approach of eddy definition using the SSHa contour succesfully tracked features through time periods in which the Okubo-Weiss determined area fell transiently below 5000 km^2, which was important for the present study.

Data from the tracking algorithm was used to identify the trajectories of the two eddies sampled during the cruise. Figure 5.10 shows the tracks formed by the weekly +10cm SSHa contours for both eddies sampled. The initial and final contours are highlighted in red for visibility. The contours for the Sitka eddy are found in the northeast GoA. Our analysis first identifies the Sitka eddy near (220.8° E, 57.5° N) in the week of 10 January 2007. The details of the trajectory are difficult to interpret purely from the figure; our description here follows from close examination of the frame-to-frame 10 cm contour evolution. Following formation, the Sitka eddy propagated initially to the north along the coast, joining with a previously distinct eddy from the south. In June, the contours veered offshore south of Yakutat Bay and southwest of CTD 4 cast (shown as a red star). In the open GoA, the eddy developed two lobes, both of which were sampled in August 2007 and visible in Figure 5.2. In late September, the 10 cm contour divided into two, and our eddy detection algorithm continued to track the southern lobe. Following detachment, this northern lobe was not automatically identified because

its duration did not meet the minimum 12 week requirement; visual inspection of the raw SSHa field revealed that the northern lobe translated to the north, weakened, and ultimately dissipated near the northern GoA shelf just west of Prince William Sound in late October or early November 2007. The southern lobe remained nearly stationary in the region of detachment until its ultimate dissolution in December 2007. We note that as discussed above, the August hydrography revealed that the northern lobe (not the southern lobe) contained the most distinct core θ-S properties, but we have no hydrographic data from late September to see how the two eddy core properties subsequently devloped. Over the course of the life of the eddy, the translational speed of the feature varied widely (between 0.3 cm/sec and 9.6 cm/sec), but its average and median values were approximately 2.2 and 1.6 cm/sec, respectively.

The description of the Kenai eddy translation is considerably simpler than that of the Sitka. This feature first appeared in water deeper than 200 m on 10-Jan-2007, off the shelf to the southwest of the Kennedy and Stevenson Entrances to Cook Inlet. It then propagated to the southwest along the shelf edge and within the Alaskan stream. The eddy center (as determined by the SSHa weighted geometric mean of positions within the 10 cm contour) veered slightly offshore southeast of Kodiak island before returning closer to the shelf. During this time, the translational speed of this eddy was also highly variable, between 0.4 cm/sec and 13.6 cm/sec; its average velocity was to the southwest at $\sim$ 2.9 cm/sec, and its median speed was 2.6 cm/sec. The eddy was still extant as of 23-Jan-2008, the last available Aviso SSHa snapshot at the time of our analysis.

The location of CTD cast 32, described above, is also shown in Figure 5.10 as the red triangle. As described above, CTD cast 32 had θ-S properties quite similar to those of the Kenai eddy core. The proximity of this cast to the initial position Kenai eddy as identified by our algorithm further supports the notion that the eddy formed in the western GoA within the Alaskan Stream and should not be classified as a more typical Yakutat, Sitka, or Haida eddy.

Chapter 4

Discussion

This study describes analysis of Sitka and Kenai eddies in the Gulf of Alaska from August 2007. Our "Sitka" eddy was sampled in the north-eastern GoA. Although its hydrography shows that the core water is similar to water at the shelf break near where it was sampled, analysis of its SSHa signature first picks it up further southeast, in the Sitka formation region. The similarity of local shelf-break water at the sampling location suggests that there may be a substantial degree of along-shore homogeneity of θ-S properties in this region. In contrast, the core water of our "Kenai" eddy has θ-S properties that are distinct from the eastern eddy, but similar to those observed at a shelf station near the Kennedy and Stevenson entrances to Cook Inlet. Furthermore, our investigation of its trajectory using satellite observations also tracks its origination point to this area. To further substantiate this likely generation spot, near the Kennedy and Stevenson entrances to Cook Inlet, we now consider possible errors in our analysis of the SSHa.

As mentioned previously, our tracking algorithm tags as separate eddies any feature that falls below the detection threshold for a timestep, but later strengthens and again exceeds the threshold. It is conceivable that the Kenai eddy was one such case, potentially linked to a feature that had formed earlier in the eastern GoA. In this case, a Hovmöller plot of SSHa following a typical propagation pathway for eddies transiting from the eastern to western GoA should reveal anomalies that are technically distinct but potentially related. A similar analysis was applied by Okkonen *et al.* (2001) to data from the GEOSAT, ERS-1, and TOPEX altimeter missions in order to identify and track the propagation of mesoscale eddies along the boundaries of the GoA.

Figure 5.11 shows the distribution of those features identified by our algorithm. Black triangles indicate where an eddy is first detected, red triangles mark the location where eddy properties fall below the critical threshold, and blue crosses track eddy centers in the intervening time. Additionally, cyan stars mark the starting locations of the two eddies we sampled. Though feature initiation occurs broadly within the eastern GoA, two clusters of black triangles are visible: one is off of the shelf in the southeast Gulf near Queen Charlotte Island (the Haida formation region), and the other is in the northeast Gulf, extending from near Sitka out to the northwest (the Sitka formation region). Haida eddies propagate both northwestward along the shelf break and often westward out into the central Gulf. While some Sitka eddies move into the interior of the Gulf, many propagate within a $1 - 2$ degree corridor along the shelf break. Another region of enhanced eddy generation is at the head of the GoA, southeast of Prince William Sound. Trajectories originating here all propagate to the west/southwest

within the Alaskan Stream. Finally, a few eddies, including our "Kenai" eddy, originate southeast of the entrance to Cook Inlet and east of Kodiak Island. These features, marked in the figure with green stars, also propagate to the southwest along the shelf break.

It is worth noting that some eddies form in the interior of the eastern Gulf away from the shelf and then propagate westward, although none of these tracks transition to the near-shelf region in the western GoA. Finally, it is striking that there is almost no eddy origination by our criteria in the interior of the western Gulf. We speculate that the termination of eddies to the east and the absence of eddies in the west (the "eddy desert" mentioned by Henson & Thomas (2008)) is related to the chain of seamounts that bisect the interior of the Gulf. These features are tall, extending to the upper 1000 m of the water column, and are visible in the bathymetric contours of the figure. A more dynamical investigation of the influence of the seamounts on eddy propagation and termination is left for a future study. Taken as a whole, this distribution of regional eddy formation and translation reinforces the view of along-shelf propagation as the primary pathway by which eddies transit from the eastern to the western GoA. For our Hovmöller diagram, we select a track that is approximately 1 degree from the 500 m isobath (the Center line in Figure 5.12). This track is roughly consistent with the region of high eddy probability presented by Henson & Thomas (2008) (their Figure 5).

Figure 5.13 shows contours of positive SSHa as a function of longitude along the central Hovmöller track in intervals of 5 cm for the last quarter of the satellite record (September 2004 through January 2008). Several sets of SSHa contours are visible at

different times and longitudes along this track. As also documented by Okkonen *et al.* (2001), their general slope of decreasing (east) longitude with increasing time indicates westward eddy propagation along the track. In the easternmost part of the record, past 225° E, one set of contours with a relatively steep slope can be seen; this feature corresponds to a Haida eddy that propagated uncharacteristically far northward along the shelf before transiting westward. Haida eddies typically detach from the shelf and propagate into the basin on a heading between 240° and 300° soon after formation, leaving signatures in the Hovmöller plot more like those seen around March 2005 and March 2007.

Between about 220 and 225° E longitude are found structures forming in the Sitka/Yakutat region. Their propagation is visibly more westward than the Haida eddies because the track for the Hovmöller diagram veers westward in this portion of the GoA. Features that emerge near 215° E originate near the head of the Gulf, south and southeast of Kayak Island, while contours that begin near 210° E correspond to those near the gap between the Kenai peninsula and Kodiak Island.

The black and red lines overlaid show the locations of the centers of the Kenai and Sitka eddies, respectively, projected onto the central Hovmöller track. The (black) line representing the center of the Kenai eddy follows the SSHa contours along this track extremely well. In addition, the time and longitude where the eddy originates closely matches the appearance of SSHa contours at that time and longitude as well. Finally, it is apparent that there is no set of SSHa contours that can obviously be identified as progenitors of the Kenai eddy. A Sitka eddy developed in winter 2006 and disappeared

in summer 2006, and its slope appears potentially continuous with that of the Kenai eddy, though 6 months and approximately 5 degrees of longitude separate these features. However, from this analysis we can say only that none of the contender eddies in the vicinity of the Kenai eddy were continous with it, nor had comparable amplitudes. As a result, we conclude that the Kenai eddy originated approximately at this location and time.

In contrast, the (red) line representing the Sitka eddy center tracks the contours of SSHa very well only until early summer 2007, when the line diverges from them over the longitude range of $216 - 218^{\circ}$ E. As mentioned previously, the Sitka eddy experienced a split into northern and southern lobes in June 2007. The (red) line in this plot corresponds to the southern lobe which moved sufficiently south of the central Hovmöller track that its longitudinal coordinate is independent from the SSHa signature along the track. Indeed this line reveals that the southern lobe propagated westward more rapidly than the northern lobe still visible in the SSHa contours.

In order to account for potential north-south variations in the propagation pathway of eddies transiting from the eastern GoA, we investigated two additional Hovmöller tracks (red and green lines in Figure 5.12) spanning a latitudinal distance of 1.5° from the central track. In addition, we included the 5 cm contour level to allow for more generous interpretations. Figure 5.14 shows the SSHa contours (in 10 cm intervals) for each track in its respective color overlaid in the same plot. Features that move closer to shore during their propagation should show overlap between SSHa contours from the central track (blue) and the near-shelf track (red). Likewise, features that move further

off-shelf should have overlap between the SSHa contours for the central track and the off-shelf track (green). For example, in the $216 - 218^\circ$ E region between about April and September 2007, SSHa contours for the off-shelf track pick up the southern lobe of the Sitka eddy and follow its previously-displayed path.

Other connections between features also can be seen. One example is a cluster of previously unremarkable small anomalies near 212° E in late 2006 that are revealed to be somewhat contiguous over a longer time-period and spatial extent. This cluster corresponds to a short-lived eddy of weak amplitude that formed south of Prince William Sound and propagated quickly to the south, where it joined a preexisting offshore high and dissipated months prior to the formation of the Kenai eddy. Also, the Sitka eddy whose propagation slope appeared potentially continuous with that of the Kenai eddy still lacks any direct linkage in SSHa in the intervening six months from summer 2006 to winter 2007. It is interesting to note that the anomaly beginning around March 2005 near 220° E, in the Sitka formation region, has a somewhat larger signature in the off-shelf track and indeed connects at the 5 cm SSHa level to subsequent features along the track to the west. Examination of the 2-dimensional SSHa fields reveals occasional offshore/onshore excursions that make these features appear and disappear from our central track.

The westward movement of the Haida eddies near 225° E can also be seen by the transition to the green contour set in this area, as the predominantly north-south orientation of the track in this region makes changes between tracks indicative of east-west motion of features. A more general feature of interest that emerges from looking at

this plot is that anomalies in the western GoA tend to have greater amounts of overlap in contours from multiple Hovmöller tracks than those in the eastern GoA, indicating a larger cross-shelf footprint.

While the formation of eddies in this region is considerably less common than formation at the well-studied Yakutat, Sitka, and Haida source regions in the Eastern GoA, the Kenai eddy we sampled was not a singular event. Based on Figure 5.11, we identify 6 eddies as having formed over the last 16 years in the region south of the Kenai Peninsula and near the Kennedy and Stevenson entrances to Cook Inlet. There are 3 additional features that are first detected in this region, but a visual inspection of the record shows them detaching from extant eddies that originated elsewhere in the GoA. As their provenance cannot be conclusively demonstrated, we excluded them from our tally of Kenai eddies. Of the 188 eddies identified in this GoA census, this number represents a small percentage (3.2%). However, of the 39 eddies that were identified as propagating along the Alaskan Stream over the 16 year period, this number represents 15.4%. Of these 39 features, we find 4 eddies that formed along the shelf between Sitka and Yakutat, 11 eddies that were generated between 215° E and 218° E near Kayak Island, 11 that developed south of Prince William Sound (west of 215° E), and 7 that formed further to the south or southwest of the Kenai eddy formation region.

Evidence from both hydrography and satellite altimetry supports the idea that the Kenai Eddy formed locally in the western GoA, in a relatively unstudied formation region south of the Kenai Peninsula and near the Kennedy and Stevenson entrances to Cook Inlet. While eddies forming in this region are infrequent, the satellite record

shows that our Kenai Eddy is not unique.

Chapter 5

Conclusion

Our original motivation for investigating Gulf of Alaska eddies was to understand the physical transports of shelf and basin waters that exchange nutrients and organisms between these regions, enhancing local biological production. Since the Alaskan Stream is bounded on one side by iron-rich shelf waters, and on the other side by the iron-limited HNLC waters of the subarctic North Pacific gyre, this makes the shelf break region in this area particularly fertile for biological production resulting from cross-shelf exchange. In the years since this work was originally published, other researchers have stepped up and expanded our picture both of the dynamics of this eddy in particular and of the impact of eddies in the Gulf of Alaska as a whole.

The Bruland Lab, drawing on data taken during the same cruise, showed that the core waters of the Kenai Eddy were substantially iron-enriched relative to water outside the eddy at the same depth (Lippiatt *et al.* (2011)), and posited 3 layers in the core that would deliver their iron to the surface waters on different timescales

(synoptic, seasonal, and interannual) via different mechanisms. This illustrated another way (aside from entrainment during propagation along the shelf break) that these eddies can serve as iron reservoirs to stimulate biological productivity in the interior of the Gulf. They also evaluated the potential of manganese as a tracer for iron, which could make obtaining in situ estimates of iron concentrations substantially easier for future research cruises. Their vertical profiles of iron and macronutrients, combined with estimates of the overall iron inventory of the Kenai Eddy, could be used to good effect in developing coupled physical-biological models of eddy dynamics, perhaps allowing better estimation of the biological impact of individual eddies over time.

This Kenai Eddy turned out to be a bit more notable than we would have predicted at the time that we sampled it–a Japanese research group sampled the same eddy two years later, in 2009, and published a paper detailing how the core water properties had changed in the intervening time (Ueno *et al.* (2012)). Their analysis of the eddy's propagation established it as the Kenai Eddy we sampled, and provided insight into the mechanisms responsible for mixing and modifying the core water of the eddy that could be applied to others in the Gulf of Alaska.

Finally, there have been several modeling studies of the mesoscale eddy field in the Gulf of Alaska that have made use of our observations (Fiechter *et al.* (2011), Fiechter & Moore (2012)) or eddy-detection methodology (Xiu *et al.* (2012)). In the case of the former, in situ eddy observations were assimilated by the model in order to better represent the impact of the eddy field on nutrient distribution and biological productivity. In the case of the latter, the model was used for an in-depth investigation

of the time-evolution of the core water properties for a specific Haida Eddy.

The efforts of these researchers have helped to quantify cross-shelf transport of water properties and nutrient concentrations by mesoscale eddies, as well as our ability to accurately model the coupled physical-biological fields in the Gulf of Alaska. There is still plenty of work to be done on a variety of related questions, such as potential mechanisms for vertical transport associated with eddies (nonlinear Ekman pumping from eddy-wind interactions is one possibility) and the impact of larger atmospheric patterns (NPGO, PDO, ENSO) on the spatial and temporal distribution of eddy-induced transport.

Whether by synthesizing the data presented here to help create a more complete understanding of eddy dynamics in the Gulf of Alaska, or by applying the eddy-detection methodology described here to the investigation of eddies in other regions (such as the California Current System), we believe that this work can serve as a basis for further fruitful inquiry by future students in the UCSC Ocean Science Department.

Table 5.1: CTD Cast Data

ID No.	Date Taken (GMT)	Lat. (° N)	Lon. (° E)	CTD Depth (db)	Nearby Eddy	Water Type
2	21-Aug-2007 15:51	59.467	220.167	90	Sitka	Shelf
3	21-Aug-2007 21:36	59.200	219.550	131	Sitka	Shelf
4	22-Aug-2007 01:56	58.933	218.940	303	Sitka	Source
5	22-Aug-2007 05:25	58.796	218.642	2030	Sitka	Transitional
6	22-Aug-2007 09:02	58.519	218.034	2027	Sitka	Core
7	22-Aug-2007 16:40	58.658	218.342	305	Sitka	Transitional
8	22-Aug-2007 21:46	58.383	217.738	304	Sitka	Core
9	23-Aug-2007 03:32	58.100	217.133	305	Sitka	Core
10	23-Aug-2007 06:22	58.241	217.435	3563	Sitka	Core
11	23-Aug-2007 16:13	57.618	217.047	299	Sitka	Core
14	24-Aug-2007 07:19	57.000	216.667	2029	Sitka	Sec. Core
15	24-Aug-2007 11:41	56.567	216.417	2027	Sitka	Sec. Core
16	24-Aug-2007 15:58	56.785	216.533	306	Sitka	Sec. Core
17	24-Aug-2007 21:34	56.300	216.249	306	Sitka	Sec. Core
19	25-Aug-2007 21:25	57.933	217.250	305	Sitka	Core
20	26-Aug-2007 03:59	58.093	216.983	2020	Sitka	Core
21	26-Aug-2007 06:50	58.259	216.725	2028	Sitka	Transitional
22	26-Aug-2007 10:01	58.425	216.466	2029	Sitka	Basin
23	26-Aug-2007 16:00	58.716	216.000	306	Sitka	Basin
32	01-Sep-2007 17:11	58.677	209.453	207	Kenai	Source
34	06-Sep-2007 21:15	55.000	206.004	1013	Kenai	Transitional
35	06-Sep-2007 23:48	54.941	205.566	1015	Kenai	Core
36	07-Sep-2007 02:15	54.891	205.132	1015	Kenai	Core
37	07-Sep-2007 04:36	54.832	204.697	1011	Kenai	Core
38	07-Sep-2007 06:55	54.783	204.267	1013	Kenai	Core
39	07-Sep-2007 09:14	54.734	203.833	1015	Kenai	Core
40	07-Sep-2007 11:31	54.675	203.400	1010	Kenai	Transitional
42	07-Sep-2007 16:12	54.574	202.533	1013	Kenai	Basin
44	08-Sep-2007 02:57	55.533	203.983	187	Kenai	Transitional
45	08-Sep-2007 05:33	55.284	204.083	530	Kenai	Core
46	08-Sep-2007 08:56	55.033	204.183	1008	Kenai	Core
47	08-Sep-2007 12:11	54.783	204.265	1005	Kenai	Core
48	08-Sep-2007 15:29	54.533	204.366	1012	Kenai	Transitional
49	08-Sep-2007 18:57	54.283	204.467	1013	Kenai	Basin
50	08-Sep-2007 22:01	54.033	204.566	1012	Kenai	Basin
51	09-Sep-2007 01:06	53.784	204.665	1015	Kenai	Basin

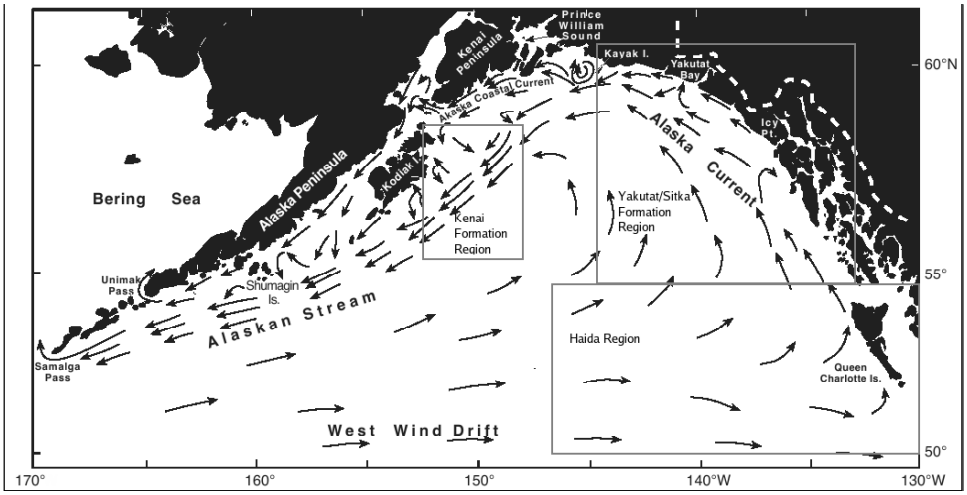

Figure 5.1: Major currents and geographical features of the Gulf of Alaska, with eddy formation regions overlaid. Adapted from Stabeno *et al.* (2004), Figure 1.

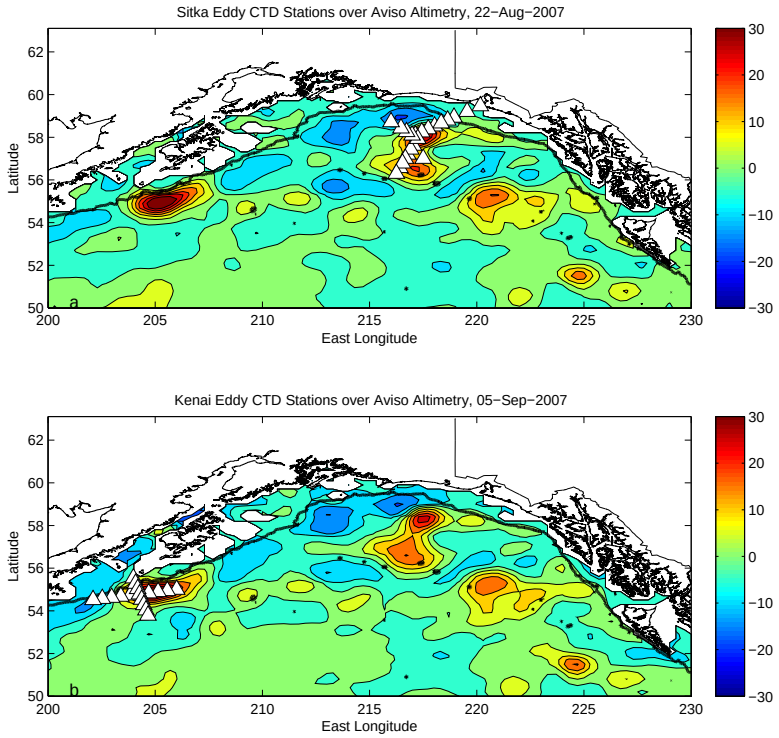

Figure 5.2: CTD cast locations for the Sitka Eddy (a) and the Kenai Eddy (b), overlaid on 5 cm contours of SSHa from Aviso altimetry, with 1000m isobath overlaid in thick black.

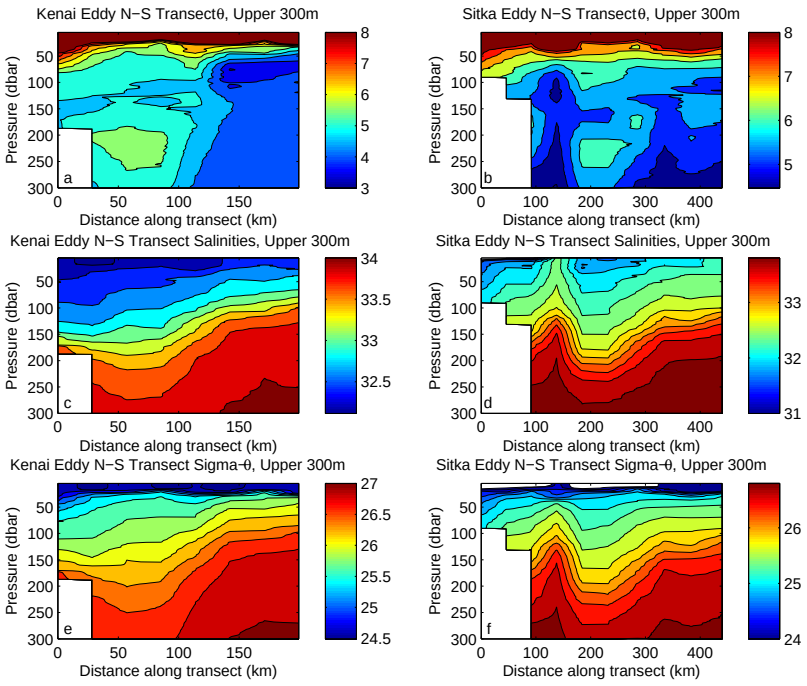

Figure 5.3: Profiles of potential temperature (a, b), salinity (c, d), and potential density (e, f) for the Kenai (a, c, e) and Sitka eddies (b, d, f), moving from on-shore (North) to off-shore (South). Note that the temperature color axis has been truncated at 8 degrees in order to emphasize subsurface structure.

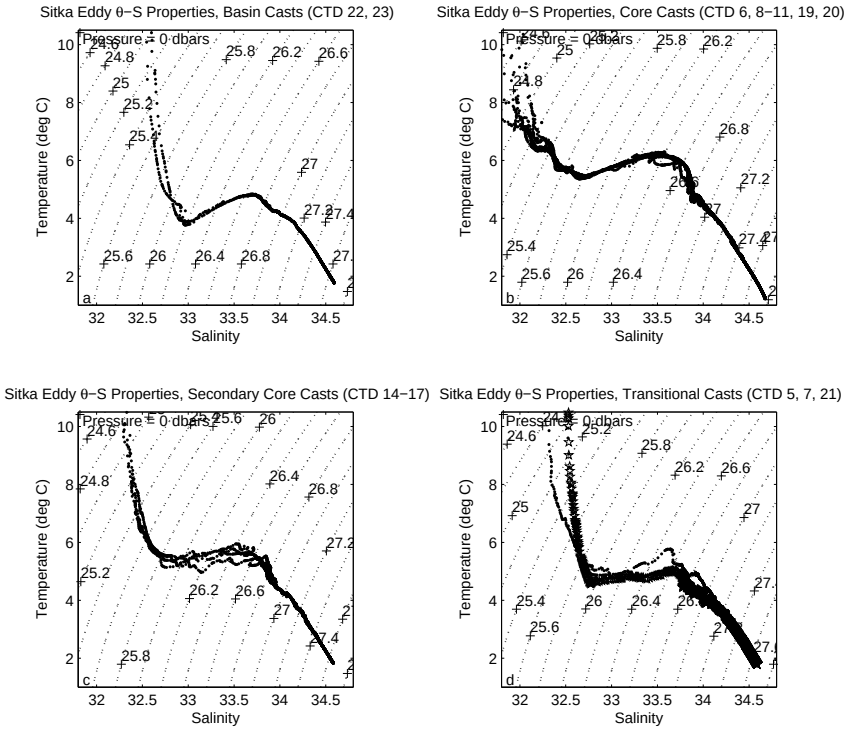

Figure 5.4: θ-S diagrams for CTD casts from the (a) Basin-like, (b) Core-like, (c) Secondary Core-like, and (d) Transitional groups for the Sitka Eddy. Groups were chosen based on a combination of θ-S structural similarity and geographical location.

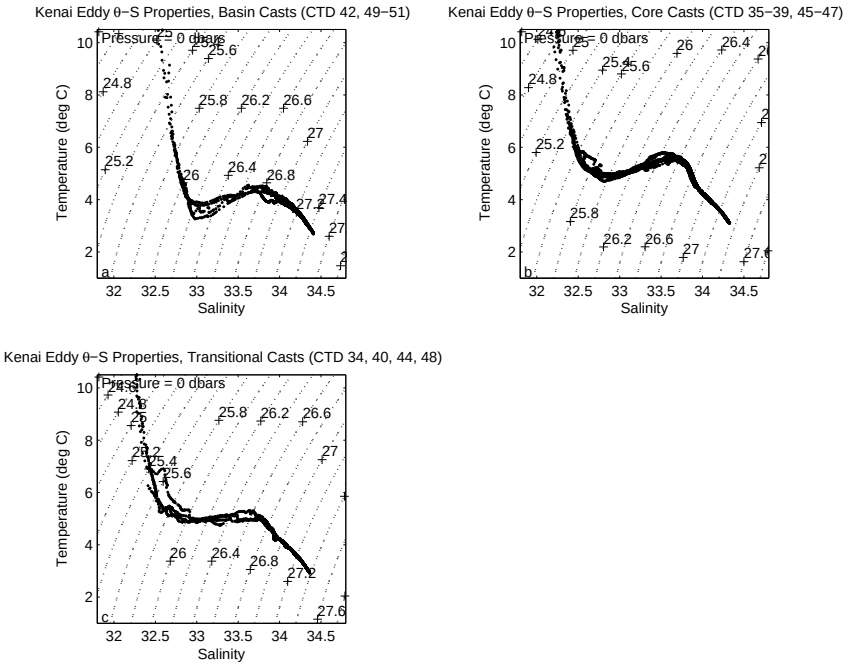

Figure 5.5: θ-S Properties by group for CTD casts from the (a) Basin-like, (b) Core-like, and (c) Transitional groups for the Kenai Eddy. Groups were chosen based on a combination of structural similarity and geographical location relative to the Kenai Eddy.

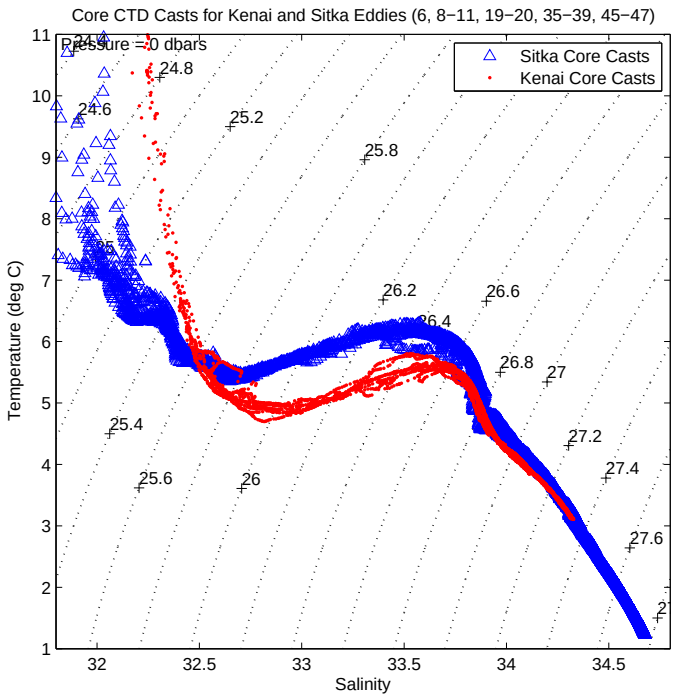

Figure 5.6: θ-S Properties for Core water from Sitka (blue) and Kenai (red) CTD casts. The shape of the curves below a salinity of about 32.5 is similar, and the magnitude of the temperature change in the $32.6 - 33.6$ range is $\sim 1°C$ in both cases. Note that the Kenai Core water over that salinity range is almost uniformly colder by $\sim 1°C$.

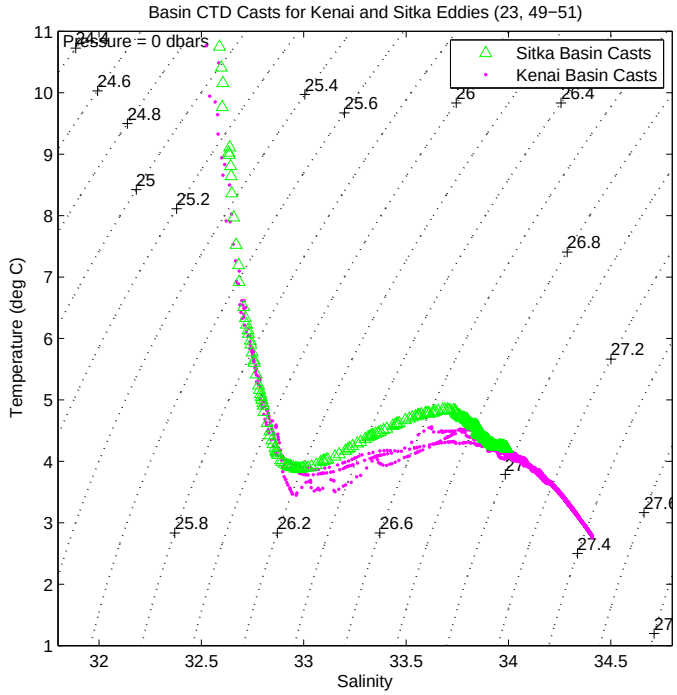

Figure 5.7: θ-S Properties for Basin water from Sitka (green) and Kenai (magenta) CTD casts. The shape of the curves below a salinity of 32.7 is similar, with the magnitude of the temperature change in the $32.7 - 33.7$ salinity range being $\sim 1°C$, although the basin water near the Kenai Eddy is colder than that near the Sitka Eddy by $\sim 0.3°C$ over that salinity range.

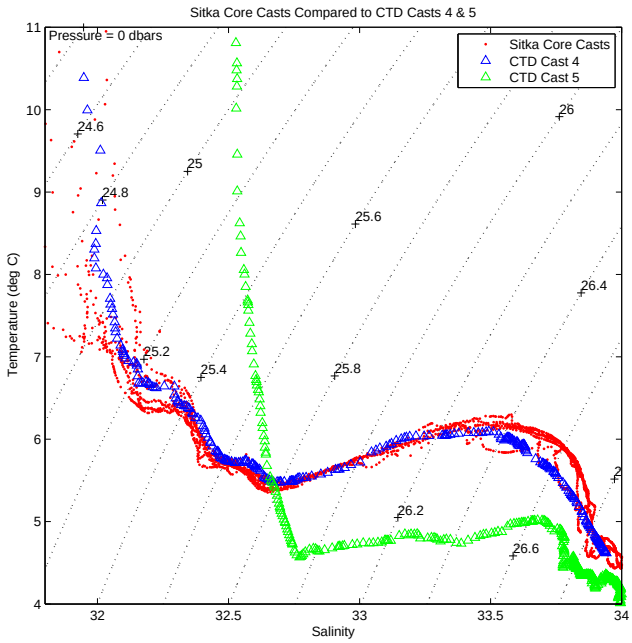

Figure 5.8: θ-S Properties of Sitka Core water (red) with CTD Cast 4 (blue) and CTD Cast 5 (green) overlaid. The Core and CTD 4 curves are almost identical in the $32.3 - 33.5$ salinity range, and exhibit a maximum divergence of approximately $0.2 - 0.3°C$ in water saltier than 33.5, suggesting nearby formation.

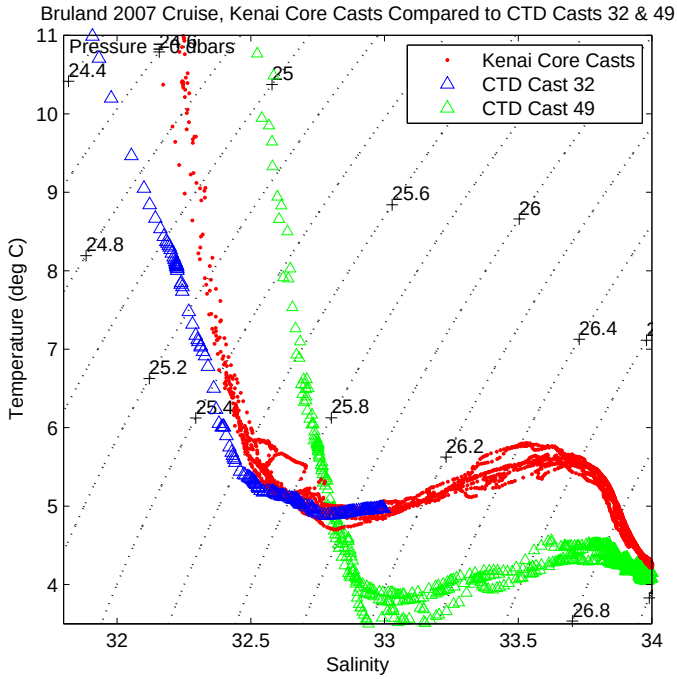

Figure 5.9: θ-S Properties of Kenai Core water (red) and CTD Cast 32 (blue), with basin CTD Cast 49 (green) overlaid for contrast. Although Cast 32 terminates at only 210 m of depth, the shape of the θ-S curve below the surface layer (salinity greater than ~ 32.5) coincides almost exactly with that of the Kenai Core Casts. This suggests that the Kenai Eddy may have formed near the location of CTD Cast 32, on the shelf by the Kennedy and Stevenson entrances to Cooke Inlet.

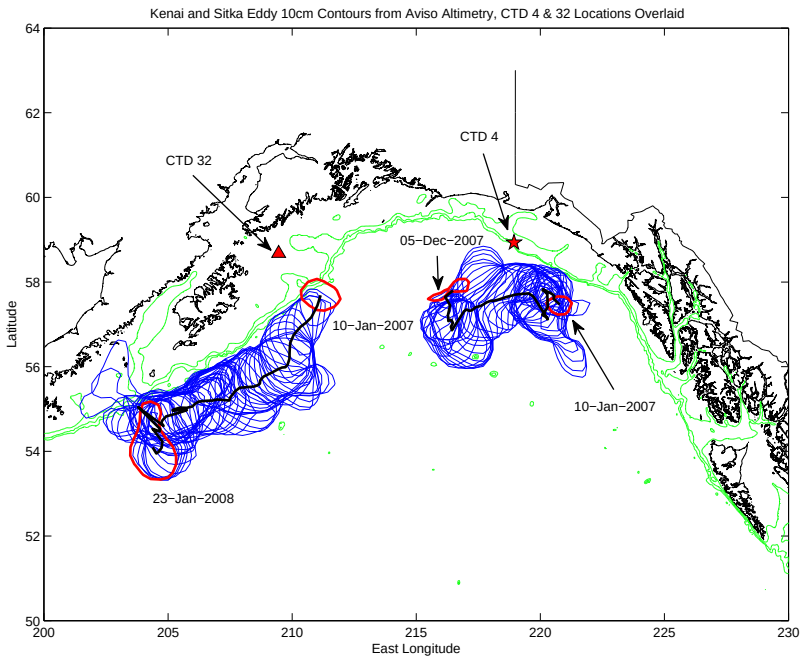

Figure 5.10: Weekly +10 cm SSHa Contours for the Kenai and Sitka eddies, with starting and ending contours labeled and outlined in red and the trajectory of the eddy center overlaid in black. The locations of CTD casts 4 (red star) and 32 (red triangle) are overlaid. Bathymetry contours for 200 m, 500 m, and 1000 m of depth are shown in green.

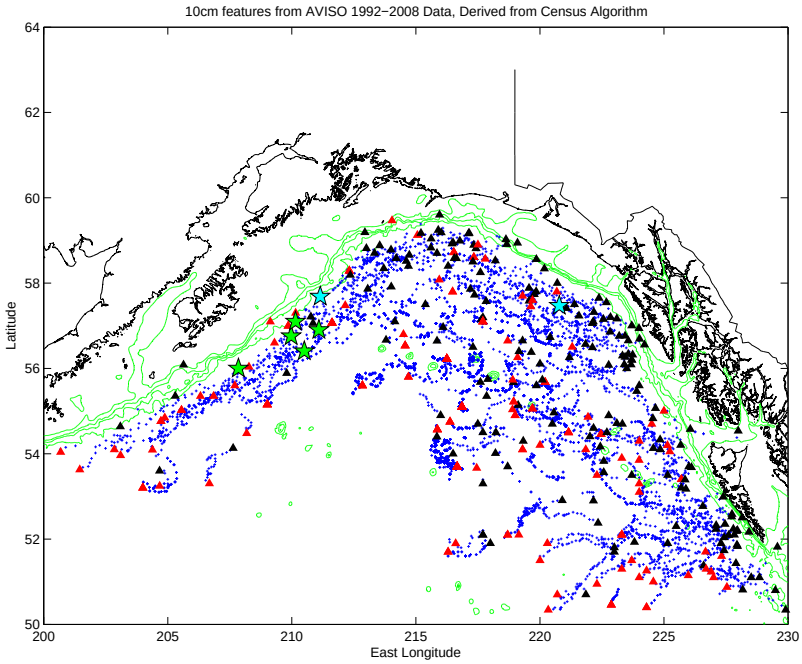

Figure 5.11: Start (black), End (red), and Interim (blue) locations of feature centers from census algorithm. Cyan stars mark the start locations of the two features sampled, while the green stars mark the start locations of the 5 other Kenai eddies identified from altimetry. Clusters of feature formation are visible near the shelf in the Yakutat, Sitka, and Haida formation regions discussed previously. The 200 m, 500 m, 1000 m, and 2000 m isobaths are overlaid in green for reference.

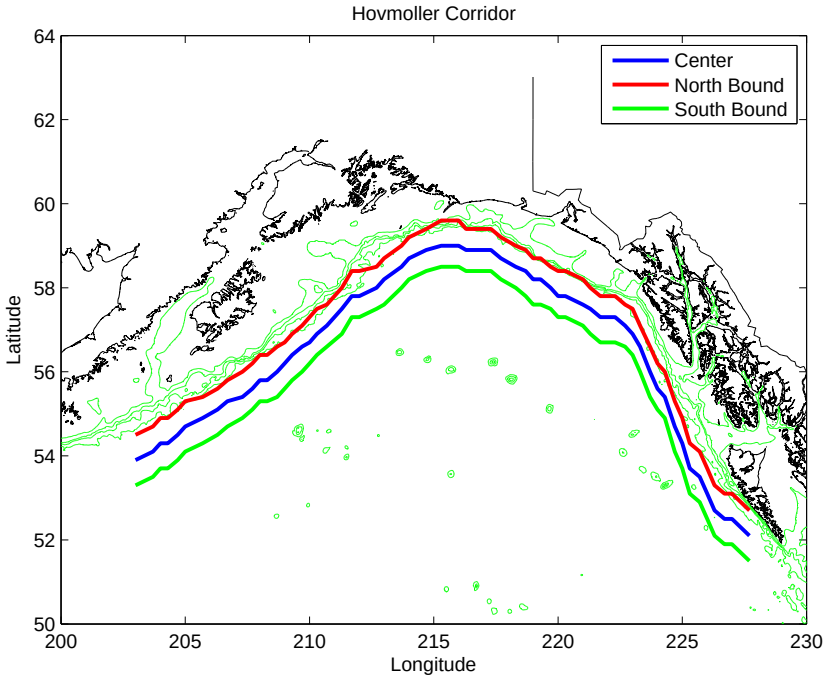

Figure 5.12: Paths for northern (red), center (blue), and southern (green) Hovmöller Tracks. Contours for the 200 m, 500 m, 1000 m, and 2000 m isobaths are displayed in green to show the location of the tracks relative to bathymetric features.

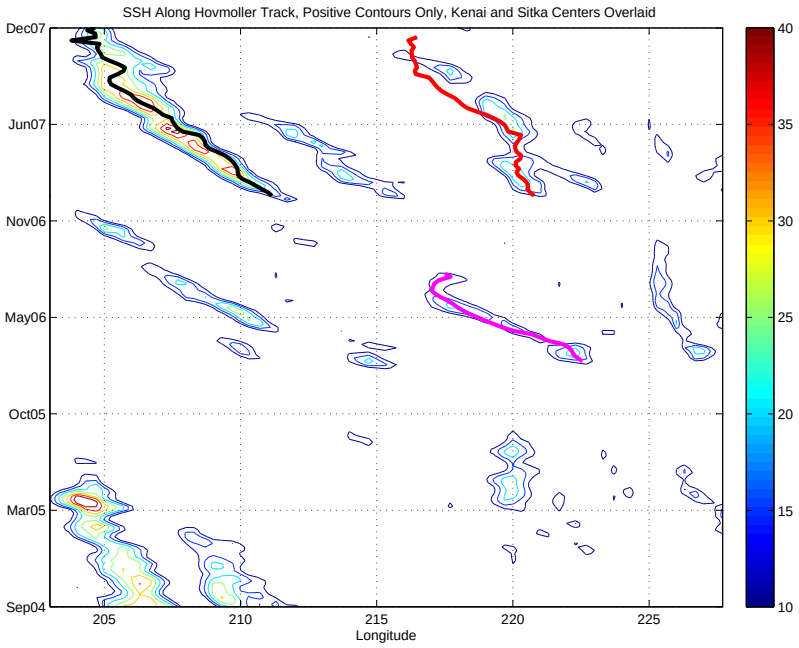

Figure 5.13: Positive SSHa Contours (5 cm interval, with first contour having a value of 10 cm) along center Hovmöller track, with Kenai (black) and Sitka (red) eddy center locations projected onto the track and overlaid. The earlier Sitka eddy mentioned in the text is also projected onto the track and overlaid in magenta.

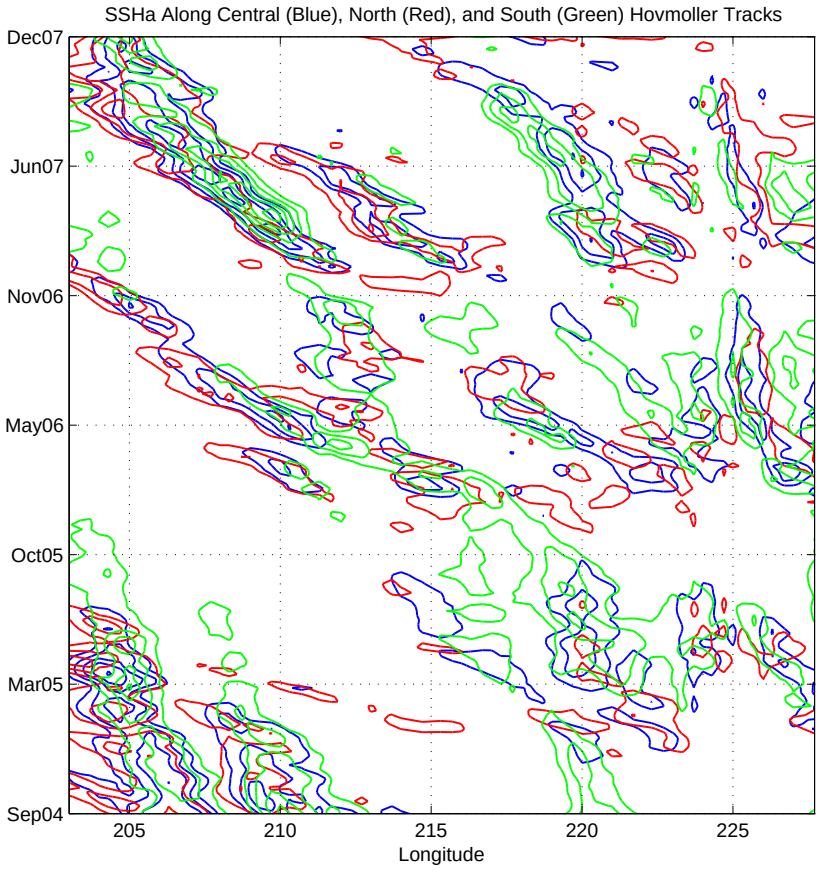

Figure 5.14: Positive SSHa Contours (10 cm interval, with first contour having a value of 5 cm) along specified Hovmöller tracks: northern (red), center (blue), southern (green).

Bibliography

Boyd, P. W., Whitney, F. A., Harrison, P. J., & Wong, C. S. 2005. The NE subarctic Pacific in winter: II. Biological rate processes. *Marine Ecology-Progress Series*, **128**, 25–34.

Chaigneau, A., Gizolme, A., & Grados, C. 2008. Mesoscale eddies off Peru in altimeter records: Identification algorithms and eddy spatio-temporal patterns. *Progress in Oceanogr.*, **79**, 106–119.

Combes, V., & Lorenzo, E. Di. 2007. Intrinsic and forced interannual variability of the Gulf of Alaska mesoscale circulation. *Progress in Oceanogr.*, **75**, 266–286.

Crawford, W. R. 2002. Physical characteristics of Haida eddies. *J. Oceanogr.*, **58**, 703–713.

Crawford, W. R., Cherniawsky, J. Y., & Foreman, M. G. G. 2000. Multi-year meanders and eddies in the Alaskan Stream as observed by TOPEX/Poseidon altimeter. *Geophys. Res. Letters*, **27**, 1025–1028.

Crawford, W. R., Cherniawsky, J. Y., Foreman, M. G. G., & Gower, J. F. R. 2002. Formation of the Haida-1998 oceanic eddy. *J. Geophys. Res.–Oceans*, **107**(C7 3069).

Crawford, W. R., Brickley, P. J., Peterson, T. D., & Thomas, A. C. 2005. Impact of Haida eddies on chlorophyll distribution in the Eastern Gulf of Alaska. *Deep Sea Res. II*, **52**, 975–990.

Cummins, P. F., & Mysak, L. A. 1988. A Quasi-geostrophic circulation model of the Northeast Pacific, Part I: A Preliminary numerical experiment. *J. Phys. Oceanogr.*, **18**, 1261–1286.

Di Lorenzo, E., Foreman, M. G. G., & Crawford, W. R. 2005. Modelling the generation of Haida Eddies. *Deep-Sea Res. II*, **52**, 853–873.

Fiechter, J., & Moore, A. M. 2012. Iron limitation impact on eddy-induced ecosystem variability in the coastal Gulf of Alaska. *J. Mar. Sys.*, **92**, 1–15.

Fiechter, J., Broquet, G., Moore, A. M., & Arango, H. G. 2011. A data assimilative, coupled physical-biological model for the Coastal Gulf of Alaska. *Dynamics Atmos. Ocean.*, **52**, 95–118.

Henson, S. A., & Thomas, A. C. 2008. A census of oceanic anticyclonic eddies in the Gulf of Alaska. *Deep-Sea Res. I*, **55**, 163–176.

Isern-Fontanet, J., Garcia-Ladona, E., & Font, J. 2003. Identification of marine eddies from altimetric maps. *J. Atmos. Ocea. Tech.*, **20**, 772–778.

Johnson, W. K., Miller, L. A., Sutherland, N. E., & Wong, C. S. 2005. Iron transport by mesoscale Haida eddies in the Gulf of Alaska. *Deep Sea Res. II*, **52**, 933–953.

Kirwan, A. D., Mcnally, G. J., Reyna, E., & Merrell, W. J. 1978. Near-surface circulation of eastern North Pacific. *J. Phys. Oceanogr.*, **8**, 937–945.

La Roche, J., Boyd, P. W., McKay, M. L., & Geider, R. J. 1996. Flavodoxin as an in situ marker for iron stress in phytoplankton. *Nature*, **382**, 802–805.

Ladd, C., Kachel, N. B., Mordy, C. W., & Stabeno, P. J. 2005. Observations from a Yakutat eddy in the northern Gulf of Alaska. *J. Geophys. Res.–Oceans*, **110**(C03003).

Ladd, C., Nordy, C. W., Kachel, N. B., & Stabeno, P. J. 2007. Northern Gulf of Alaska eddies and associated anomalies. *Deep Sea Res. I*, **54**, 487–509.

Lippiatt, S. M., Brown, M. T., Lohan, M. C., & Bruland, K. W. 2011. Reactive iron delivery to the Gulf of Alaska via a Kenai eddy. *Deep Sea Res. I*, **58**, 1091–1102.

Mackas, D. L., & Galbraith, M. D. 2002. Zooplankton distribution and dynamics in a North Pacific eddy of coastal origin: 1. Transport and loss of continental margin species. *J. of Oceanogr.*, **58**, 725–738.

Martin, J., Gordon, R., Fitzwater, S., & Broenkow, W. 1989. VERTEX: Phytoplankton/iron studies in the Gulf of Alaska. *Deep Sea Res., PartA*, **36**, 649–680.

Matthews, P. E., Johnson, M. A., & O'Brien, J. J. 1992. Observation of mesoscale ocean features in the Northeast Pacific using GEOSAT radar altimetry data. *J. Geophys. Res.–Oceans*, **97**, 17829–17840.

Musgrave, D. L., Weingartner, T. J., & Royer, T. C. 1992. Circulation and hydrography in the northwestern Gulf of Alaska. *Deep Sea Res.*, **39**, 1499–1519.

Okkonen, S. R., Jacobs, G. A., Metzger, E. J., Hurlburt, H. E., & Shriver, J. F. 2001. Mesoscale variability in the boundary currents of the Alaska Gyre. *Cont. Shelf Res.*, **21**, 1219–1236.

Okkonen, S. R., Weingartner, T. J., Danielson, S. L., Musgrave, D. L., & Schmidt, G. M. 2003. Satellite and hydrographic observations of eddy-induced shelf-slope exchange in the northwestern Gulf of Alaska. *J. Geophys. Res.*, **108(C2)**(3033).

Peterson, T. D., Whitney, F. A., & Harrison, P. J. 2005. Macronutrient dynamics in an anticyclonic mesoscale eddy in the Gulf of Alaska. *Deep Sea Res. II*, **52**, 909–932.

Stabeno, P. J., & Reed, R. K. 1991. Recent Lagrangian measurements along the Alaskan Stream. *Deep Sea Res.*, **38**, 289–296.

Stabeno, P. J., Bond, N. A., Herman, A. J., Kachel, N. B., Mordy, C. W., & Overland, J. E. 2004. Meteorology and oceanography of the northern Gulf of Alaska. *Cont. Shelf Res.*, **24**, 859–897.

Suga, T., Motoki, K., & Aoki, Y. 2004. The North Pacific Climatology of Winter Mixed Layer and Mode Waters. *J. Phys. Oceanogr.*, **34**, 3–22.

Swaters, G. E., & Mysak, L. A. 1985. Topographically-induced baroclinic eddies near a coastline, with applications to the Northeast Pacific. *J. Phys. Oceanogr.*, **15**, 1470–1485.

Tabata, S. 1982. The anticyclonic, baroclinic eddy off Sitka, Alaska in the Northeast Pacific Ocean. *J. Phys. Oceanogr.*, **12**, 1260–1282.

Thomson, R. E., & Gower, J. F. R. 1998. A basin-scale oceanic instability event in the Gulf of Alaska. *J. Geophys. Res.*, **103**, 3033–3040.

Ueno, H., Yasuda, I., Itoh, S., Onishi, H., Hiroe, Y., Suga, T., & Oka, E. 2012. Modification of a Kenai eddy along the Alaskan Stream. *J. Geophys. Res.*, **117**.

Whitney, F., & Robert, M. 2002. Structure of Haida eddies and their transport of nutrient from coastal margins in the NE Pacific Ocean. *J. Oceanogr.*, **58**, 715–723.

Whitney, F. A., Crawford, W. R., & Harrison, P. J. 2005. Physical processes that enhance nutrient transport and primary productivity in the coastal and open ocean of the subarctic NE Pacific. *Deep Sea Res. II*, **52**, 681–706.

Willmott, A. J., & Mysak, L. A. 1980. Atmospherically forced eddies in the Northeast Pacific. *J. Phys. Oceanogr.*, **10**, 1769–1791.

Xiu, P., Chai, F., Xue, H., Shi, L., & Chao, Y. 2012. Modeling the mesoscale eddy field in the Gulf of Alaska. *Deep Sea Res. I*, **63**, 102–117.